Gain Subsidence Method for Compensating Hole Burning from Wavelength Reconfiguration in Metro-Scale Networks

Sumaiya Binte Ali*, Dmitrii Briantcev*, Shuang Xie*, Dan Kilper*
*School of Engineering, CONNECT Centre, Trinity College Dublin, Ireland
alisu@tcd.ie, briantcd@tcd.ie, xiesh@tcd.ie, dan.kilper@tcd.ie

***Abstract*—Dynamic wavelength provisioning in ROADM-based metro networks can induce significant power excursions on existing channels due to spectral hole burning (SHB) in erbium-doped fiber amplifiers (EDFAs). This paper introduces an SHB-aware control method that mitigates SHB-induced power excursions using a single amplifier-level gain-tilt compensation adjustment under constant-gain operation. Proof of concept laboratory experiments on a 50-km link with cascaded ROADMs show that the applied gain subsidence reduces power excursions by up to 85% and 10–50% when measured after the first and second span respectively.**

***Index Terms*—Spectral hole burning (SHB), Power excursion, WDM networks, Dynamic wavelength provisioning.**

I. Introduction

Management of data flows between metro data centers increasingly involves services that occupy one or more wavelengths, motivating the use of wavelength reconfiguration over time [1]. Dynamic wavelength reprovisioning in the metro area and on inter-data center links has been proposed for emerging edge AI applications such as agentic model tuning and future 6G high-capacity connectivity [2]. While digital twins and quality of transmission optimization methods have been studied to enable rapid wavelength reconfiguration [1], dynamic power effects such as spectral hole burning (SHB) remain an impediment to rapid and stable reconfiguration.

To limit power excursions and minimize disruption to neighboring channels, wavelength provisioning is often performed on single channels using gradual power adjustments that can be very time consuming depending on the number of elements that require tuning [1], [3]. While rapid provisioning can be done with minimal impact, depending on the conditions of the network, wavelength dependent EDFA gain dynamics can lead to pronounced power excursions that accumulate over cascaded spans and extend beyond the existing channels, perturbing neighboring channels across the spectrum and even resulting in power instabilities in mesh networks [4]–[6].

In our previous experimental work on a metro-scale multi-ROADM path, we observed that rapid and simultaneous switching of multiple channels in a wavelength band can produce power excursions exceeding 6.3 dB, with the magnitude of the excursion strongly dependent on the spectral location of the added wavelengths [7]. In particular, provisioning within the short wavelength range of the C-band (approximately 1530–1535 nm), where SHB is strongest, results in significantly larger excursions, affecting both newly added channels and surviving channels in a wider portion of the band [7]–[9]. From an operational perspective, this behavior effectively renders certain spectral regions unfavorable for dynamic allocation operations, as provisioning in these regions can destabilize power across the entire C-band and impact provisioned services [8], [10].

SHB is an amplifier phenomenon arising from residual inhomogeneous broadening of the erbium gain medium, leading to wavelength dependent gain depletion due to localized saturation. Prior analytical and experimental studies have established that SHB dynamics depend on pump wavelength, pump power, and spectral loading, and that SHB-induced gain deformation along a path can accumulate large channel power reductions across cascaded EDFAs [5], [11], [12]. As a result, SHB has been extensively studied, primarily with the objective of accurately predicting wavelength dependent gain behavior under given operating conditions [8], [10], [13]. Alongside these modeling efforts, mitigation techniques have also been explored at the amplifier level, including hybrid gain-controlled EDFA designs and amplifier-intrinsic self-compensation approaches based on controlled pump distribution [14], [15].

However, these studies largely consider SHB under stationary loading or controlled laboratory conditions and do not explicitly address how SHB-driven gain dynamics manifest as power excursions during operational wavelength provisioning events. Prior studies rely on detailed amplifier knowledge, novel EDFA designs, or fine-grained actuation mechanisms. More recently, machine-learning methods have been used to characterize wavelength dependent EDFA gain for predictive purposes, but have not been used to mitigate the impact of SHB [16], [17]. In metro optical networks, wavelength provisioning is typically initiated at a single node, with limited visibility into changing conditions across the remaining spans of the link, which often self-tune locally on short time scales and receive only global corrective tuning over longer time scales. Under such partial observability and localized control, mitigation strategies must operate with incomplete information and rely on a small number of simple and available control parameters.

Motivated by these constraints, in this work, we introduce an SHB-aware gain subsidence process that estimates the

978-3-903176-78-2 © 2026 IFIP

EDFA pre-amplifier gain tilt to be applied in order to mitigate SHB-induced power excursions on existing channels arising from the addition of new channels prior to provisioning. The method uses the estimated SHB depth and estimates the maximum power excursion that may arise during wavelength provisioning, from which an appropriate amplifier tilt adjustment is selected. Rather than relying on post-provisioning WSS channel rebalancing or coordinated retuning of multiple amplifiers, the method addresses the operational burden of changing many control settings by using only a simple, rapid adjustment of the EDFA gain-tilt control at the pre-amplifier of the first span. In this way, it shows that a single amplifier-level adjustment can substantially reduce problematic SHB-induced power excursions during rapid reconfiguration.

II. Gain Subsidence Algorithm

Channel power excursions in transmission systems, corresponding to a persistent deviation from the desired channel power, originate from the wavelength dependent gain of optical amplifiers and accumulate across successive spans. In conventional operation, such excursions are corrected through wavelength dependent attenuation at the multiplexing stages (WSS), which rebalances channel powers without altering the wavelength dependent gain profile of the amplifiers. As a result, any gain-induced spectral imbalance will accumulate along the transmission line, at the cost of increased wavelength dependent variation of the relative ASE noise and non-linear effects. Adjusting the gain tilt of the line amplifiers can instead directly reshape the wavelength dependent gain response, enabling a reduction in the magnitude of accumulated power excursions induced by channel reconfiguration, illustrated in Fig. 1(c). This approach is particularly relevant in practical reconfiguration scenarios where channels are provisioned as a band between two endpoints, such as high-capacity data-center interconnect services [18]. In multi-domain or operationally constrained environments [19], compensation must often be initiated from a single accessible node, with no access to downstream attenuation settings or intermediate amplifiers. Under these constraints, adjusting the gain tilt of an accessible line amplifier offers a practical way to influence channel interactions along the transmission path without disrupting existing flattened power or mean-gain regulation.

To implement this compensation in a practical and repeatable scenario, Algorithm 1 estimates the SHB-induced excursion expected for a given added-channel configuration and selects a corresponding pre-amplifier tilt adjustment. The algorithm uses separate preliminary measurements of the maximum depth of the hole burning effect, which is a characteristic of the amplifier's maximum SHB depth as an empirical input parameter. For this study, a representative value of $D_{\max} = 0.7$ dB, obtained from separate preliminary measurements at $\lambda_{\text{SHB}} = 1532$ nm for an added-channel count of $N_{\max} = 10$, is used in the computation. The estimated hole-burning depth depends on the number of added channels, corresponding to the total added-channel power, and on the spectral location of the added-channel band. The formula is an empirical approximation of the behavior observed in separate measurements using added-channel counts $N \in \{1, 3, 5, 8\}$ at different center wavelengths

Algorithm 1 SHB-Aware Gain Subsidence (pseudocode)

Input: added channel-band center wavelength λ_C; CUT (pre-existing) channel count N_{CUT}; added channel count N_{add}; wavelength-spread parameter σ_λ; the center wavelength for hole burning effect λ_{SHB};maximum depth $D_{\max}$ N_{add} channel count at which $D_{\max}$ is observed $N_{\max}$;Tuning factor k; amplifier count M;tilt bounds $[T_{\min}, T_{\max}]$

Output: $t^\star$

Depth D over added band:

$$D(\lambda_C, N_{\text{add}}) \leftarrow \frac{D_{\max} \exp\left(-\frac{(\lambda_C - \lambda_{\text{SHB}})^2}{\sigma_\lambda}\right)}{|N_{\text{add}} - N_{\max} + 1|}$$

Estimate maximum power excursion (accumulated over M amplifiers):

$$E_{\max} \leftarrow 10M \log_{10}\left(\frac{D(\lambda_C, N_{\text{add}}) + N_{\text{CUT}}}{N_{\text{add}} + N_{\text{CUT}}}\right)$$

Compute raw compensating tilt:

$$t_{\text{raw}} \leftarrow -k\, E_{\max}$$

Apply tilt bounds $[T_{\min}, T_{\max}]$:

$$t^\star \leftarrow \max\big(T_{\min},\, \min(T_{\max},\, t_{\text{raw}})\big)$$

return $t^\star$

Given the estimated hole burning depth D, the algorithm then estimates the worst-case CUT power excursion $E_{\max}$ using the loading ratio between the added channels N_{add} and the pre-existing (CUT) channels N_{CUT}, with accumulation over M cascaded amplifiers. The tilt setting $t^\star$ is then selected as $-kE_{\max}$ and constrained to the allowable range $[T_{\min}, T_{\max}]$. The tuning factor k is set to 1 here, but can be adjusted depending on how aggressive the operator would like to make the adjustment. In this case, large values of k are not used in order to avoid negative excursions. The resulting estimated tilt values are shown in Fig. 4 as markers on the measured performance curves, indicating the operating points selected by the estimator.

The core principle of the algorithm is to mitigate the impact of successive hole burning along a path by creating a subsidence on the gain spectrum that induces an opposing effect to the hole burning. It takes advantage of the fact that hole burning is localized to the short wavelength end of the spectrum, and therefore tilting the gain of an amplifier creates a subsidence from the SHB region toward the long-wavelength region, where large excursions occur. While an alternative might be to apply either pre-emphasis or post-compensation adjustments directly to the channels, this requires careful measurement and tuning of individual channels to avoid further negative impacts. Directly adjusting the channels being added at the input WSS would have an opposite effect, deepening the hole burning and creating larger excursions. By contrast, post compensation still incurs the penalties due to the power excursions along the path prior to compensation. Ideally one would like to apply the gain compensation to each amplifier

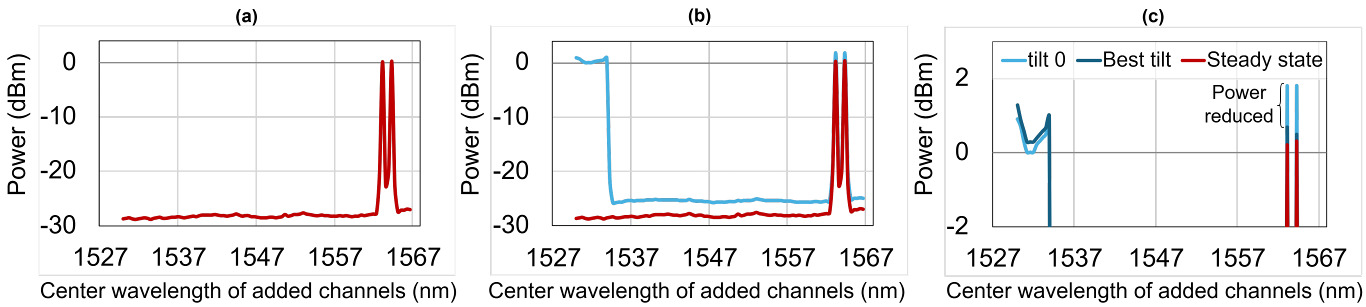

Fig. 1. Optical channel monitor (OCM) measurements of the spectrum at the output of the first span for combination-4 operation: (a) steady state operation with CUTs only; (b) grouped channel addition causing spectral hole burning and power excursions of the CUTs; and (c) application of amplifier gain tilt at the first span, suppressing CUT power excursions.

TABLE I
CHANNEL UNDER TEST COMBINATIONS

Combination	Center Wavelengths (nm)	Channel Numbers
1	1537.5, 1535.9	76,80
2	1565.9, 1537.5	3,76
3	1548.4, 1547.2	48,51
4	1564.4, 1563.2	7,10

along the path of the channels being added. However, this can be time-consuming and requires careful consideration of the changing channel configurations as other channels add and drop at intermediate nodes along the path. To simplify the control and allow for rapid reconfiguration, the gain compensation is applied to a single amplifier. The pre-amplifier following the first transmission span is selected (shown in Fig. 2). As this amplifier compensates for amplifiers along the entire transmission path, locations closer to the midpoint of the transmission path are preferred to allow some deviation to accumulate before applying the compensation and therefore avoid overcompensation. We avoid using the booster amplifiers as they operate at high output power and are carefully controlled to set the power launched into the transmission spans. This allows the steady state power management system controls to continue to operate normally.

III. EXPERIMENTAL SETUP

In order to study the effectiveness of this power excursion compensation technique, experiments are conducted on a metro-scale ROADM transmission system [20]. Based on previous results, adding channels in a band up to 10 channels to a line system with only one or two existing channels along the same path can be considered an extreme case, susceptible to large power excursions. A group of 10 channels, upon addition, will create a deep localized hole in the short-wavelength gain region. The relatively higher power of the 10 added channels compared to the existing channels results in very large excursions that are typically positive as the automatic gain controls adjust for the depletion due to SHB. A total of four combinations of CUT placement were selected to cover a representative set of spectral scenarios, spanning shorter wavelengths, longer wavelengths, mid-spectrum, and mixed spectral regions, as summarized in Table I. The added 10-channel block was first swept across the C-band in order to identify the spectral region that produce strong SHB-induced excursion behavior. Based on this sweep, the short-wavelength SHB-sensitive cases were selected and are shown in Fig. 3 for gain subsidence evaluation. For the quantitative tilt-performance comparison of Fig. 4, one representative added-channel center wavelength near 1531.6 nm was used across all CUT combinations. The configuration consisting of 10 added channels co-propagating with two existing channels at different spectral locations is therefore selected to assess the performance of the proposed gain subsidence algorithm. We also note that the presence of additional channels that add and drop along the path, or higher numbers of pre-existing channels, would reduce the magnitude of the observed power excursions. Thus, the selected configuration serves as a worst-case scenario that provides an initial proof-of-concept.

As illustrated in Fig. 2, two 200 Gb/s DP-16QAM coherent signals, generated by ADTRAN TeraFlex transceivers, and a broadband amplified spontaneous emission (ASE) source used to create a WDM comb, were injected through MUX ports of a Lumentum WSS-based ROADM. After spectral multiplexing at the ingress MUX, the signals were launched into a multi-span amplified transmission link with a launch power of approximately 0 dBm per channel at the fiber input. At the end of the transmission link, the signals were connected directly to their receive ports to evaluate their performance.

The link consists of cascaded ROADM nodes interconnected by 25 km standard single-mode fiber spools, forming a total 50 km metro-scale network. Each node integrates wavelength-selective DEMUX/MUX stages with pre-amp (P) and booster (B) EDFAs. All EDFAs, in this case, were operated in constant-gain mode under internal automatic power control. Throughout the experiment, gain tilt adjustments were applied exclusively at the pre-amplifier of the first transmission span. The gain tilt in this case depends on the amplifier inversion level and is adjusted through the amplifier's internal tilt-control mechanism, implemented by changing the setting of

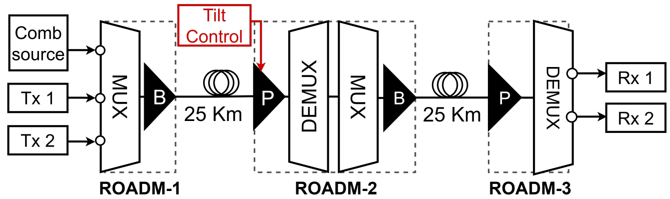

Fig. 2. Experimental ROADM-based metro network setup with cascaded amplified spans

an internal VOA. All remaining amplifiers were operated with their default zero-tilt configuration to isolate the effect of the proposed single-point compensation.

Prior to any reconfiguration measurements, the line system was initialized under fully loaded conditions, with all wavelength channels present across the C-band to provide an attenuation reference during reconfiguration. The optical power spectrum was flattened by adjusting the per-channel attenuation at the wavelength selective switch (WSS) MUX and DEMUX stages, resulting in a uniform (flat) launch power of 0 dBm at the span. After full-load initialization, only CUTs were propagated through the link (shown in Fig. 1(a)), which was used as the baseline steady state for all subsequent measurements. All baseline measurements were performed with zero applied spectral tilt across the network, corresponding to the default operating condition of the ROADM and EDFA control loops. Optical channel monitors at each ROADM were used to verify stable CUT power levels along the link, while receiver-side measurements of Q-factor and OSNR were recorded to establish reference performance prior to any reconfiguration. After this initial spectral flattening, no additional WSS attenuation changes were used as the mitigation mechanism during the reconfiguration experiments; the applied compensation was implemented only through EDFA gain-tilt adjustment at the pre-amplifier of the first span.

Starting from the CUTs-only steady state, a contiguous block of ten channels was introduced in a single reconfiguration step at the ingress MUX at a specific center wavelength as mentioned. A number of tilt settings ranging from 0 to -5 dB were then applied iteratively at the pre-amplifier of the first span to measure the resulting power excursion impact on the existing channels. Figure 4 shows the measured excursion mapping together with the estimated tilt value.

IV. Results

The results presented in this section involve two distinct phases: pre-provisioning tilt estimation and post-provisioning performance validation. Prior to channel provisioning, the algorithm estimates an appropriate gain subsidence tilt. Importantly, this estimation is performed without access to receiver-side signal quality metrics; the selected tilt is therefore based solely on power redistribution behavior rather than on Q-factor optimization.

After channel provisioning, the network response is used to validate the pre-tilt estimation. In the worst-case configuration considered here, a contiguous block of ten channels is introduced in the short-wavelength SHB-sensitive region. Figure 3 shows the measured OCM spectra after the last transmission span for the four CUT-placement combinations. Relative to the steady state baseline, placing the added 10-channel band in this short-wavelength region produces a strong localized hole, which is accompanied by positive power excursions on the pre-existing CUTs. The gain subsidence traces show that applying negative amplifier tilt reduces the magnitude of these excursions, although the amount of suppression depends on the spectral location of the CUTs relative to the added-channel band.

The corresponding measured CUT power excursions are quantified in Fig. 4, which plots excursion magnitude as a function of applied gain tilt for the four CUT-placement combinations. The baseline operating point corresponds to the steady state with zero applied tilt. Under zero tilt, ten added channels induce pronounced wavelength dependent gain redistribution, resulting in significant CUT power excursions. After the first transmission span, the peak excursions are approximately 2 dB. After the second span, these excursions increase further due to accumulation across cascaded amplifiers, reaching values between 2.3 and 4 dB. The associated increase in received power leads to higher OSNR and Q-factor compared to the CUT-only baseline; however, this operating point arises from unregulated gain redistribution and is therefore unfavorable from a power-stability perspective under dynamic reconfiguration.

Applying a negative gain tilt (from 0 to -5 dB) at the pre-amplifier of the first transmission span produces a systematic reduction in power excursion for all CUT placements, confirming gain subsidence as an effective local control mechanism for mitigating spectral hole burning (SHB)–induced excursions. Using a single common operating point, the proposed algorithm selects a tilt of -2.3 dB (indicated by star markers in Fig. 4) as a compromise setting that suppresses the maximum excursion while avoiding excessive negative undershoot in the first span for configurations that cross below 0 dB at stronger tilt magnitudes. The estimated tilt value is wavelength dependent; thus it is the same across all combinations as the added channel position was kept the same for simplification of this experiment.

For CUT placements located away from the most strongly depleted SHB region (e.g., combinations 3 and 4), this operating point reduces first-span excursions to near-zero levels, corresponding to reductions of up to 85%. In contrast, CUTs located adjacent to the added channel block (combination 1 and the short-wavelength CUT in combination 2) exhibit more limited suppression, typically in the range of 20–45%, consistent with the stronger local gain depletion at those wavelengths. Although the gain subsidence adjustment is applied only at the first-span pre-amplifier, it also limits the accumulation of wavelength dependent gain redistribution across cascaded amplifiers, leading to second-span excursion reductions of approximately 10–50%, depending on CUT placement.

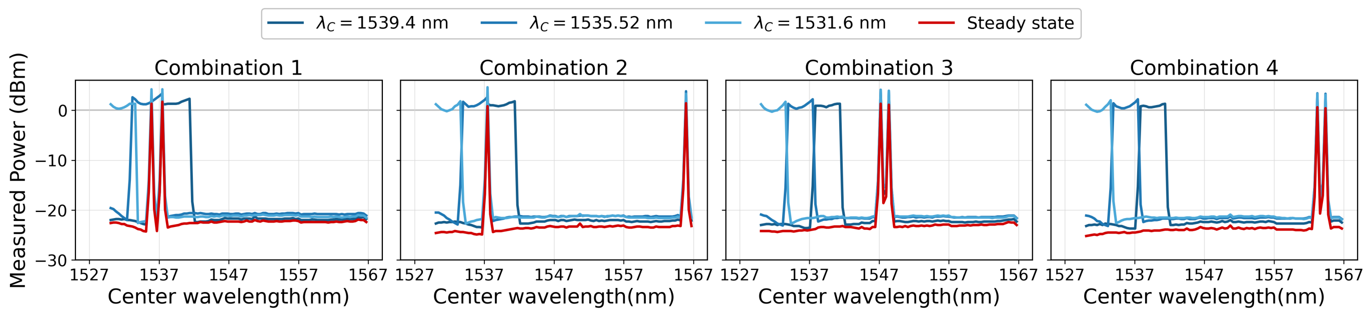

Fig. 3. Measured OCM spectra after the last transmission span for the four CUT-placement combinations. The traces correspond to different center wavelengths λ_C of the added 10-channel band and the steady-state baseline.

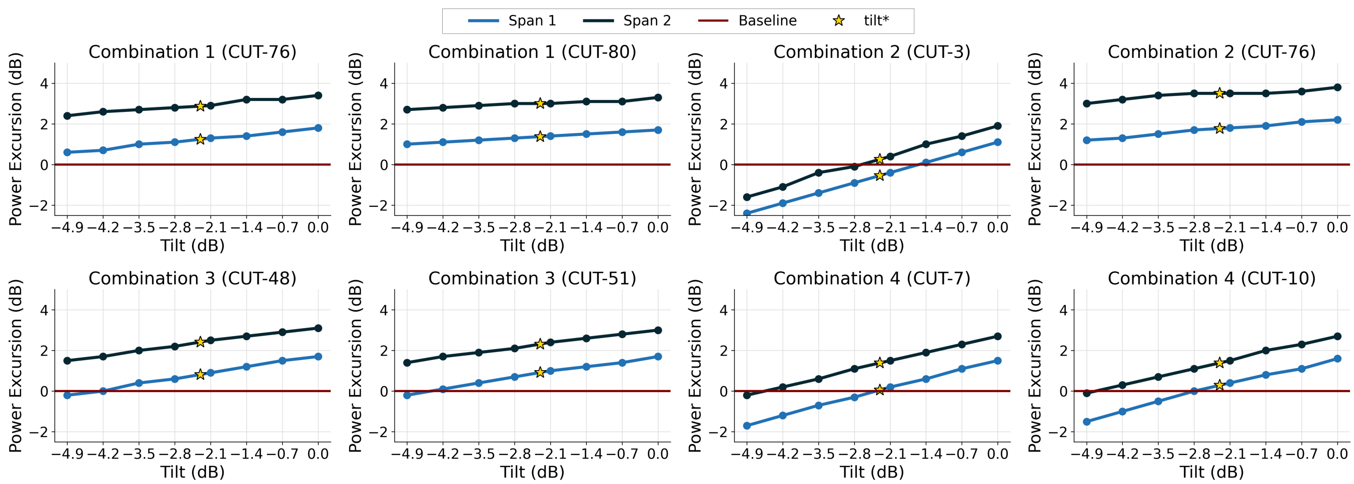

Fig. 4. Measured channel-under-test power excursions when channels were added at a center wavelength of $\lambda_C = 1531$ nm, plotted versus applied gain tilt for different spectral placements across two spans; star markers indicate the algorithm-selected tilt adjustment $t^\star = -2.3$ dB.

In addition to excursion magnitude, the receiver-side Q-factor is monitored after reconfiguration to verify that the application of gain subsidence does not introduce a service penalty. For all CUT combinations, the zero-tilt reconfiguration case yields a higher measured Q than the steady state baseline (e.g., increasing from approximately 11.7–11.8 dB to $\sim$12.3 dB), consistent with positive power excursions temporarily boosting the received OSNR. After applying the estimated negative gain tilt, the excursions are suppressed and the corresponding worst-case Q remains close to the baseline value, with the maximum observed penalty limited to ≤ 0.5 dB. These results confirm that although the tilt is selected prior to provisioning and without knowledge of Q, the resulting operating point maintains the signal quality. Of course, for a short metro link such as this, the impact on Q is not expected to be large and the more important impact is the large change in power, which is shown to be reduced in all cases as described above.

The results further indicate that the proposed gain subsidence compensation has limited effectiveness for certain CUT configurations. In particular, channels located immediately adjacent to the edge of the added channel block continue to exhibit relatively large positive excursions, as they coincide with the steepest local gain depression associated with SHB and therefore experience only weak benefit from the imposed subsidence. Such unfavorable placements are predictable from the spectral loading configuration and can be mitigated or avoided through provisioning-aware design choices. Further investigation is required to fully characterize the limits of this approach across a broader range of reconfiguration scenarios, including different numbers of cascaded spans and amplifiers, as well as more heterogeneous channel loading conditions along the transmission path, and will be the subject of future work.

V. Conclusion

Experiments conducted on the simultaneous provisioning of multiple channels in metro-scale amplified optical communication links demonstrated amplifier gain subsidence for mitigating SHB-induced power excursions. An algorithm was introduced for estimating the SHB hole depth impact over a transmission path and determining the subsidence amplitude to apply at a single amplifier control point. Applying this algorithm at the pre-amplifier after the first transmission span was shown to alter the accumulated gain profile across four amplifiers and two transmission spans, creating a subsidence across the gain band that reduces the impact of the SHB. The excursions created by adding 10 channels in a band in the SHB gain region to two channels placed at different spectral locations were systematically reduced across all tested channel placements. Measured Q-factors remained within 0.5 dB of baseline, confirming that excursion suppression did not introduce a noticeable service penalty. Future work should extend to a wider range of channel configurations and longer multi-span and mesh topologies.

Acknowledgment

The work was supported by Science Foundation Ireland grant #13/RC/2077_P2 and by Research Ireland grant 22/FFP-A/10598. It was also supported by the European Commission project ECO-eNET, which has received funding from the Smart Networks and Services Joint Undertaking (SNS JU) under grant agreement No. 10113933.

References

[1] H. Nishizawa et al., "Fast WDM provisioning with minimal probing: The first field experiments for DC exchanges," J. Opt. Commun. Netw., vol. 16, no. 2, pp. 233–242, 2024, doi: 10.1364/JOCN.505729.

[2] R. Raj, D. Dass, K. Kaeval, S. Patri, V. Sleiffer, B. Baeuerle, W. Heni, M. Ruffini, C. Browning, A. Naughton, R. Mackey, D. Mackey, B. Vukovic, J. Smajic, J. Leuthold, C. Natalino, L. Wosinska, T. Svensson, A. Kaszubowska-Anandarajah, I. Mesogiti, S. Pryor, A. Tzanakaki, R. Nejabati, P. Monti, and D. Kilper, "Towards efficient confluent edge networks," in Proc. Joint European Conf. on Networks and Communications & 6G Summit (EuCNC/6G Summit), 2024, pp. 1163–1168, doi: 10.1109/EuCNC/6GSummit60053.2024.10597093.

[3] J. Junio, D. C. Kilper, and V. W. S. Chan, "Channel power excursions from single-step channel provisioning," J. Opt. Commun. Netw., vol. 4, no. 1, pp. A1–A7, 2012.

[4] D. J., H. Patil, and B. S. Halakanimath, "Impact of power transients on optical amplifier characterization and performance in long-haul transmission systems," in Proc. Int. Conf. Optimization Computing and Wireless Communication (ICOCWC), 2024, pp. 1–6.

[5] J. T. de Araujo, A. Carbo Meseguer, and J.-C. Antona, "Experimental model of EDFA spectral hole burning for WDM transmission systems," in Proc. Optical Fiber Communications Conf. and Exhibition (OFC), 2023, pp. 1–3, doi: 10.1364/OFC.2023.M2E.1.

[6] D. C. Kilper, C. A. White, and S. Chandrasekhar, "Control of Channel Power Instabilities in Constant-Gain Amplified Transparent Networks Using Scalable Mesh Scheduling," J. Lightwave Technol., vol. 26, no. 1, pp. 108–113, Jan. 2008.

[7] S. Ali, F. Slyne, A. Raj, D. Dass, and D. Kilper, "Hole-burning mediated dynamics for channel band reconfiguration in metro ROADM systems," in Proc. IEEE Future Networks World Forum (FNWF), 2024, pp. 560–565, doi: 10.1109/FNWF63303.2024.11028830.

[8] I. L. Rittner and P. M. Krummrich, "Physical model approach for the spectral hole burning characteristics of erbium-doped fiber amplifiers," in Proc. Photonic Networks, 21st ITG-Symposium, 2020, pp. 1–5.

[9] I. L. Rittner and P. M. Krummrich, "Modelling spectral hole burning of EDFA assuming a small number of distinct groups of erbium ions," in Proc. Photonic Networks, 24th ITG-Symposium, 2023, pp. 1–8.

[10] F. Yaman, A. D'Amico, E. Mateo, T. Inoue, and Y. Inada, "Machine learning model for EDFA predicting SHB effects," in Proc. European Conf. on Optical Communication (ECOC), 2024, pp. 272–275.

[11] M. Holtmannspoetter and B. Schmauss, "Dynamic model of spectral hole burning for EDFAs with 980-nm pumping," in Proc. Optical Fiber Communication Conf. and Exposition (OFC/NFOEC), 2011, pp. 1–3.

[12] L. Rapp and J. Ferreira, "Dynamics of spectral hole burning in EDFAs: Dependency on pump wavelength and pump power," IEEE Photon. Technol. Lett., vol. 22, no. 16, pp. 1256–1258, 2010, doi: 10.1109/LPT.2010.2052798.

[13] I. L. Rittner and P. M. Krummrich, "Verification of the physical modelling approach of spectral hole burning in EDFA based on erbium ion groups," in Proc. Optical Fiber Communication Conf. (OFC), 2024, Paper W2A.24.

[14] J. C. R. F. Oliveira, A. F. Herbster, J. R. F. Oliveira, A. A. Juriollo, and A. C. Bordonalli, "Minimization of gain error due to spectral hole burning using HGC-EDFA with generalized dynamic gain range," in Proc. SBMO/IEEE MTT-S Int. Microwave and Optoelectronics Conf. (IMOC), 2009, pp. 846–849.

[15] L. Wang, Y. Lan, M. Sharma, X. Peng, and Z. Jiang, "Self-compensation of spectral hole burning effect in super C-band EDFA," in Proc. Optical Fiber Communication Conf. (OFC), 2023, Paper Th3C.6.

[16] F. da Ros, U. C. de Moura, and M. P. Yankov, "Machine learning-based EDFA gain model generalizable to multiple physical devices," in Proc. European Conf. on Optical Communication (ECOC), Brussels, Belgium, 2020, pp. 1–4, doi: 10.1109/ECOC48923.2020.9333297.

[17] A. Mahajan, K. Christodoulopoulos, R. Martínez, S. Spadaro, and R. Muñoz, "Modeling EDFA gain ripple and filter penalties with machine learning for accurate QoT estimation," J. Lightwave Technol., vol. 38, no. 9, pp. 2616–2629, May 2020, doi: 10.1109/JLT.2020.2975081.

[18] T. Mano, T. F. de Lima, Y.-K. Huang, Z. Wang, W. Ishida, E. Ip, A. D'Amico, S. Okamoto, T. Inoue, H. Nishizawa, V. Curri, G. Zussman, D. Kilper, T. Chen, T. Wang, K. Asahi, and K. Takasugi, "First field demonstration of automatic WDM optical path provisioning over alien access links for data center exchange," in Proc. Eur. Conf. Optical Communications (ECOC), 2023, pp. 234–237, doi: 10.1049/icp.2023.2048.

[19] K. Anazawa, T. Inoue, T. Mano, K. Obana, E. Oki, and H. Nishizawa, "First Demonstration of an SDN Controller for Optical-Circuit-Switched Datacenter Networks," in Proc. IEEE Opto-Electronics and Communications Conference (OECC), 2024, pp. 1–3.

[20] Open Ireland Testbed Wiki, "Open Ireland Testbed," Open-Ireland-Testbed documentation, https://open-ireland-testbed.github.io/wiki/ (accessed Dec. 2025).